IRAQI JOURNAL OF MATERIALS
Volume (3) Issue (3) July-September 2024, pp. 17-24

Terahertz Lasing Using Optically Excited Neutral Donor Centres Embedded in Crystalline Silicon

Miroslav Makarov, Alexander Timoshkov, Anatoly Borisov

Department of Physics, Faculty of Science, Technical University of Sofia, Sofia, BULGARIA

Abstract
In this work, the results demonstrate with the evidence the possibility to get the THz lasing using optically excited neutral donor centres embedded in crystalline silicon. The physical principles are clear and on the whole the results of the theoretical calculations taking into account both the intravalley and intervalley phonon-assisted captured carrier relaxation are in a good qualitative agreement with the experimental data, particularly for the Si:P laser. At the same time the experiment with Si:Bi revealed an unexpected delay (3×10^{-7} s) in the temporal behavior of the stimulated emission.

Keywords: Silicon devices; Laser; Shallow centers; Stumulated emission
Received: 20 February 2024; **Revised:** 21 May 2024; **Accepted:** 28 May 2024; **Published:** 1 July 2024

1. Introduction
Silicon based semiconductors and semiconductor heterostructures are promising media for THz laser engineering due to the highly developed technology of silicon growth and doping, low level of lattice absorption in THz range and different ways to obtain the population inversion of charged carriers.

Historically there were several attempts to make a THz laser using intraband optical transitions in silicon. In 1979 the idea of the mechanism of the population inversion and the amplification on the transitions between light (*l*) and heavy (*h*) holes subbands of the valence band in crossed electric and magnetic ($E\perp H$) fields was proposed [1]. Since that time hot hole silicon lasing is under discussions.

Monte-Carlo calculations predicted small signal gain of 0.1 cm^{-1} on intersubband *l-h* optical transitions in Si in $E\perp H$ in the frequency range of 50-230 cm^{-1} [2]. Later it was shown that Landau level optical transitions in $E\perp H$ fields can also provide the amplification of THz radiation on the light hole cyclotron resonance (at frequency of 26 cm^{-1} at H=3T) [3,4]. In this case the required inversion population and nonequidistancy of principle Landau levels are provided due to the mixing (hybridization) of light and heavy subband states. The above mentioned laser mechanisms were successfully achieved experimentally in *p*-Ge in the frequency range of 50-140 cm^{-1} [5,6]. However, similar experimental investigations of silicon met the problem of the breakdown of the acceptors at liquid helium temperature and because of this reason was not successful. Nevertheless, positive results concerning hot hole gain in $E\perp H$ fields in silicon have been obtained recently [4].

The idea to use optically excited neutral shallow donors (D^0) for THz lasing was proposed for the first time in 1996 [7,8]. It was reported that both acoustic phonon (Si:P) and optical phonon (Si:Bi) assisted relaxation of non-equilibrium carriers under the photoionization of donors by CO_2 laser radiation leads to population inversion and the amplification on intracentre transitions for moderate level of doping ($N_D\approx10^{15}$ cm^{-3}) and low lattice temperatures ($T\leq$ 30-60 K). Later on, the theoretical model was worked out more precisely [9,10] taking into account multivalley structure of the conduction band. It was shown that the intervalley phonon assisted nonradiative transitions are very important for quantitative analysis.

Up to the moment THz lasing has been realized and laser transitions have been unambiguously identified for phosphorus-doped (Si:P) [11-13], bismuth-doped (Si:Bi) [13,14] and antimony-doped (Si:Sb) [15] silicon.

In this article, recent theoretical calculations and experimental investigations concerning THz lasing of group V shallow donor centres under their photoionization by CO_2 laser radiation are reviewed and discussed.

2. Theoretical background

Shallow donor states in silicon are originating from the six equivalent valleys (v= 1-6) along <100> orientations in the energy structure $E_v(\mathbf{k})$ of the conduction band (see review [16]). Also, all bound impurity states except of the lowest *1s* state can be considered using a single valley effective mass theory. In the frame of such approach every state of the Coulomb centre exhibits at least a six-fold degeneracy originating from conduction band minima. However for the *1s* ground state the effective-mass theory is inadequate and the degeneracy is lifted by the crystal cell potential. The overlapping of the *1s* eigenfunctions belonging to each valley leads to the intervalley interaction (hybridization of states) and as a result to the valley orbit splitting of the *1s* state. The effect depends on the chemical nature of the impurity atom and is called the "chemical splitting". The binding energies of the bound states of group V donors (arsenic As, antimony Sb, phosphorus P, bismuth Bi) as well as lithium Li donor are presented in Table (1). One can see that the *1s* multiplet resolves into a triplet $1s(T_2)$, a doublet *1s(E)* and a singlet $1s(A_1)$.

Table (1) Energy levels of group V and lithium donors in silicon [16]

Level	P	As	Sb	Bi	Li	Theory
$1s(A_1)$	45.59	53.76	42.74	70.98	31.24	31.27
1s(E)	32.58	31.26	30.47			31.27
$1s(E+T_2)$					33.02	31.27
			32.89	32.89		
$1s(T_2)$	33.89	32.67				31.27
			32.91	31.89		
$2p_0$	11.48	11.50	11.51	11.44	11.51	11.51
2s		9.11		8.78		8.83
$2p_\pm$	6.40	6.40	6.38	6.37	6.40	6.40
$3p_0$	5.47	5.49	5.50	5.48	5.49	5.49
3s				4.70		4.75
$3d_0$	3.83	3.8		3.80		3.75
$4p_0$	3.31	3.31	3.33	3.30	3.32	3.33
$3p_\pm$	3.12	3.12	3.12	3.12	3.12	3.12
4s				2.89		2.85
$4f_0$	2.33			2.36		2.33
$4p_\pm$, $5p_0$	2.19	2.19	2.20	2.18	2.20	2.19, 2.23
$4f_\pm$	1.90	1.90	1.94	1.91	1.90	1.89
$5f_0$	1.65		1.71	1.67	1.64	1.62
$5p_\pm$	1.46	1.46	1.48	1.46	1.47	1.44
$5f_\pm$	1.26				1.25	1.27
$6p_\pm$	1.09	1.07	1.10	1.08	1.07	1.04

Moreover for the substitution donors P, As, Sb, Bi the $1s(A_1)$ state is a ground state. It is shown below that donor lasing arises on the $2p_0 \rightarrow \{1s(E), 1s(T_2)\}$ allowed optical transitions in the frame of a four level scheme. Consequently the "chemical splitting" determines the laser states and is a major factor in the formation of the population inversion and the amplification of the donor transitions.

There are two mechanisms of the population inversion of donor states in silicon under photoexcitation. The first one is connected with the low temperature intracentre acoustic phonon assisted relaxation and is based on the accumulation of charged carriers in the long-living $2p_0$ state of P, Sb, As and perhaps Li neutral donor centres. For *n*-type Si active optical phonons have energies about 63 meV and 59 meV, which are larger than the binding energies of P, Sb, As and Li impurity states (see Table 1). Therefore for these donors at low lattice temperature ($T< 30$ K) the electron-phonon interaction mediated by optical lattice vibrations is negligible and the population of the donor states under the optical excitation (Fig. 1) is controlled by acoustic phonon emission.

The matrix elements of such processes decrease with the increasing of the energy gap ΔE between corresponding levels provided $qa>1$, where a is an effective radius of the state orbit, q is a wave-vector of the phonon required for the nonradiative transition. Note, that for the long-wavelength acoustic phonons participated in the intravalley intracentre relaxation $\hbar qs = \Delta E$, where *s* is a speed of sound, $\hbar$ – Plank's constant. At the condition *qa*>1 the phonon-assisted transitions are ended outside of the *q*-space area where the wavefunctions of these states are mainly localized and the rate of the intravalley relaxation is suppressed with increasing *qa* parameter. As a consequence the step-by-step cascade acoustic phonon relaxation is slowing down and transitions between adjacent levels predominate at least for the lower ($n \leq 3$) bound states. Moreover, the lifetime of the $2p_0$ state occurs to be the longest.

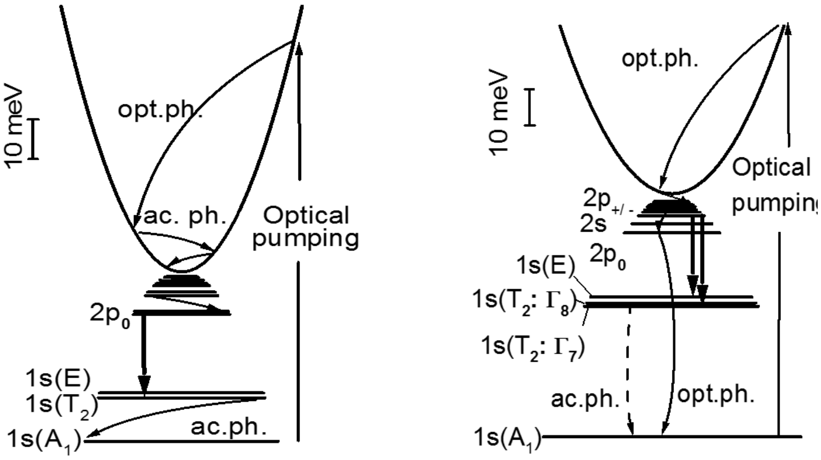

Fig. (1) The energy levels scheme and possible radiative and nonradiative transitions in Si:P (left) and Si:Bi (right) under the optical pumping

The estimation made in the frame of the single valley approximation gives the lifetime of the $2p_0$ state equal to 1.5×10^{-8}s. Therefore, the majority of excited carriers passes through the $2p_0$ state before the returning to the ground state and is accumulated there. In comparison the lifetime of the *1s(E)* state is much shorter (2×10^{-10}s) because of the smaller energy gap between this state and $1s(A_1)$ ground state. Thus the four-level laser scheme (Fig. 1) with thresholdless population inversion on the $2p_0 \rightarrow 1s(E)$ transitions can be realized. However the problem connected with a trapping of carriers on the $1s(T_2)$ state is expected within single valley approximation. On the base of group theory analysis of electron-phonon interaction [17] it was revealed that the acoustic phonon assisted intravalley relaxation is forbidden for this state. The accumulation of carriers on the $1s(T_2)$ states terminates the inversion population and the laser effect. Fortunately, the intervalley relaxation from the $1s(T_2)$ state is allowed and makes the lifetime of the $1s(T_2)$ state comparable with the lifetime of the *1s(E)* state. Besides this, the intervalley scattering decreases the lifetime of the $2p_0$ state to 10^{-9}s [10]. Thus, it can be concluded that both inter- and intravalley acoustic phonon assisted transitions are important and have to be taken into account in the theoretical model. The results of the calculation of the involved states populations, free carrier concentration *n* and the small signal gain within the single valley approximation and with the account of the intervalley phonon assisted transitions for phosphorus donors are presented in Fig. (2) and on Fig. (3) correspondingly for comparison.

The absorption of the THz radiation by the negatively charged donor centres (D^-) [18] created by a CO_2 laser photoionization has also been taken into account. It is shown that the typical threshold flux density for laser action is of the order of 10^{23} quantum$\times$cm$^{-2}\times$s^{-1} for the uncompensated samples. The optimal doping level, 10^{15}-3×10^{15} cm^{-3}, is determined by the two factors: maximum of the active centres on the one hand and, on the other hand, minimum of the impurity concentration broadening of the linewidth for the intracentre laser transition. It should be emphasised that the compensation ($K=N_d/N_a$, where N_d and N_a is the donor and acceptor concentration correspondingly) level influences the gain essentially due to the changing the absorption by the D^- centres (Fig. 4).

In contrast to silicon doped by phosphorus , where population inversion is based on the long-living $2p_0$ state, in silicon doped by bismuth the inversion is formed due to the resonant interaction with intervalley optical phonons (Fig. 1). The $2p_0$ and *2s* states in Si:Bi are coupled to the $1s(A_1)$ state via optical phonon emission [19] and have a very short lifetime, of about 1 ps. Due to this coupling the majority of the optically excited electrons relaxes directly to the ground state and, therefore, does not reach the *1s(E)* and $1s(T_2)$ states. As a result, the population of the *2s* and $2p_0$ states as well as *1s(E)* and $1s(T_2)$ states is relatively low.

The lifetime of the $2p_\pm$ state (10^{-10} s) is not longer than that of *1s(E)*, $1s(T_2)$ states (10^{-9} s), controlled by intravalley acoustic phonon assisted transitions. Nevertheless, due to the fact that the probability for excited carrier to reach the $2p_{\pm}$ state (0.5) is much higher then that of *1s(E), 1s(T₂)* states (~10³) the inverse population is formed between the $2p_{\pm} \rightarrow 1s(E), 1s(T_2)$ as well as on both $2p_{\pm} \rightarrow 2p_0$ and $2p_{\pm} \rightarrow 2s$ transitions.

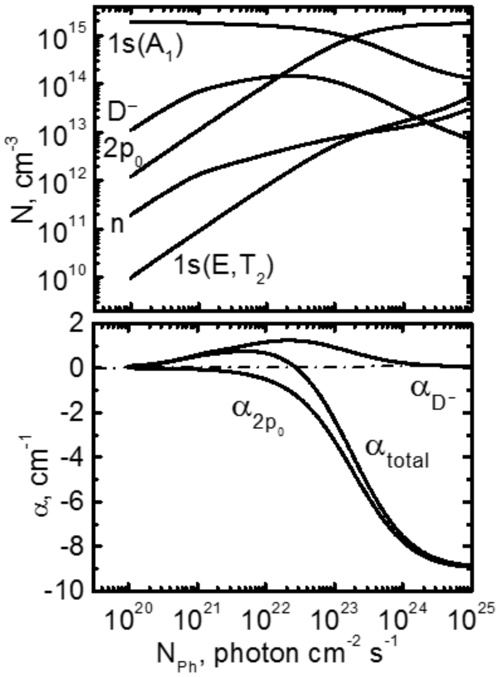

Fig. (2) The populations of donor states (upper graph) and absorption/amplification coefficient (lower graph) of Si:P calculated in the frame of single valley approximation for $2\times10^{15}cm^{-3}$ and low compensation (0.002) versus 10.6 μm photon flux density N_{Ph}

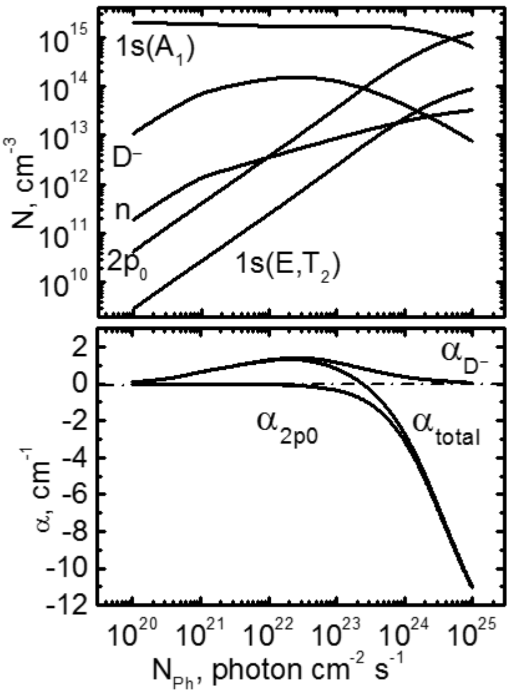

Fig. (3) The populations of donor states (upper graph) and absorption/amplification coefficient (lower graph) of Si:P calculated in the frame of intervalley approximation for $2\times10^{15}cm^{-3}$ and low compensation (0.002) versus 10.6 μm photon flux density N_{Ph}

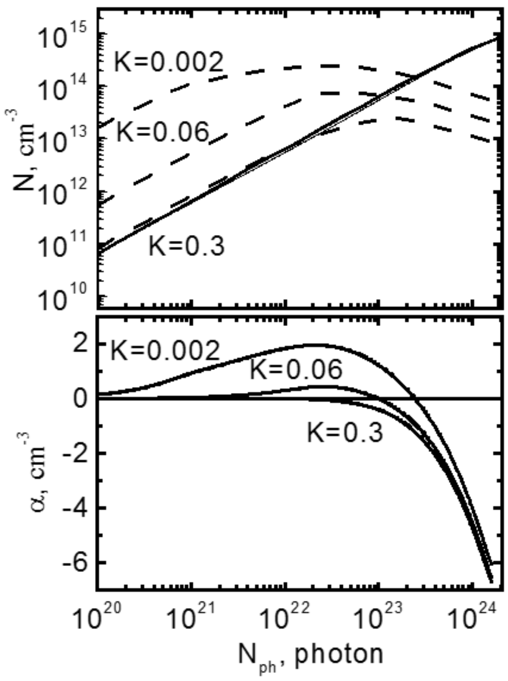

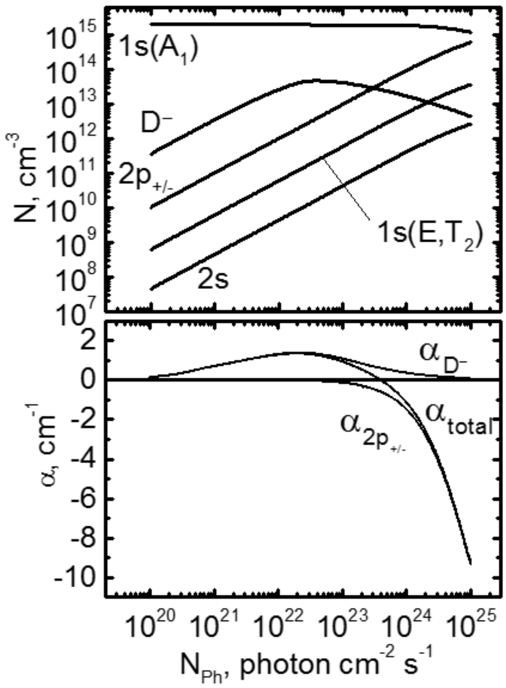

Fig. (4) The $2p_0$ (solid) and D^- centre (dash) population (upper graph) and absorption/amplification coefficient (lower graph) for different levels of compensation versus 10.6 µm photon flux density N_{Ph}

Fig. (5) The populations of donor states (upper graph) and absorption/amplification coefficient (lower graph) of Si:Bi calculated in the frame of intravalley approximation for 3×10^{15}cm^{-3} and compensation 0.1 versus 10.6 µm photon flux density N_{Ph}

Thus a four-level laser scheme can be realized from Bi donor transitions. The larger gain is expected on transitions from the $2p_\pm$ to the *1s(E)* and $1s(T_2)$ states (Fig. 1). Calculations of the level populations and gain made using probability technique are presented on the *Figure 5*. The transition rates were estimated within the frame of the hydrogen-like centre model for D^0 centre states [20] and the zero-radius potential model for D^- centre states (neutral centre with an extra electron [18]). The lasing threshold value in Si:Bi (10^{24} photons$\times$cm$^{-2}\times$s^{-1}) is higher than that in Si:P due to the difference of the lifetimes of the $2p_\pm$ and $2p_0$ states.

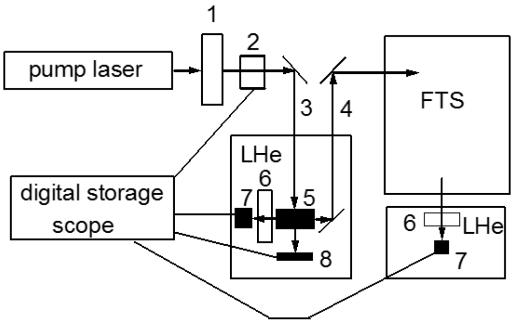

Fig. (6) Experimental setup: (1) attenuator, (2) CO_2 drag detector, (3) pump beam, (4) silicon emission beam, (5) silicon sample, (6) THz filter, (7) and (8) Ge detectors

3. Experiment

Low compensated (K< 0.01) Si:P, Si:Sb and Si:Bi samples were grown by the float zone procedure with simultaneous incorporation of the doping elements from the melt. The dominant donor concentrations in these samples are in the range of (0.1-12)$\times10^{15}$ cm^{-3}. Additionally, the Si:P crystals with $K \leq 0.3$ were prepared by neutron transmutation doping [21]. Samples with different doping concentrations were cut in form of rectangular parallelepipeds (typical crystal dimensions are 7$\times$7$\times$5 mm^3) from the Si ingot and then polished to provide a high-*Q* resonator on internal reflection modes. The Si samples with the low doping concentration (ca. 10^{14} cm^{-3}) were used to identify the dominant impurity as well as the concentration of the incorporated electrically active centres by absorption spectroscopy.

The samples were mounted in a holder, which was immersed in a liquid helium (LHe) vessel (Fig. 6). A grating tunable TEA CO_2 laser with a peak output power up to 1.6 MW in the wavelength range 9.2-10.7 µm was used as the pump source. The THz emission from the optically pumped samples was registered by a LHe cooled Ge:Ga photodetector inside the same vessel. To prevent irradiation of the detector by the CO_2 laser, 1 mm thick sapphire filters were placed in front of the detectors. The pulses were recorded by the 500 MHz - bandwidth digital storage scope. For the spectral measurements the THz emission was guided by a stainless steel lightpipe into a Fourier transform spectrometre (FTS) and focused onto another LHe cooled Ge:Ga detector inside a separate cryostat. The spectrometre had a step-scan control, allowing to average the emission signal over the defined number of pulses.

Spontaneous emission was detected with the Ge:Ga detector for various pump wavelengths from the silicon doped by phosphorus, antimony and bismuth. A linear dependence of the spontaneous emission signal on the pump photon flux density up to 6$\times10^{23}$ cm^{-2}s^{-1} was found.

All Si:P samples doped higher than 5$\times10^{14}$ cm^{-3} showed spontaneous emission when pumped by a CO_2 laser. The spontaneous emission increases with increasing doping concentration. For these samples stimulated emission was observed for doping concentration in the range (0.8-5)$\times10^{15}$ cm^{-3}. The neutron transmutation doped samples, which are heavily compensated, have some significant differences. First of all, the spontaneous emission is significantly higher than for the uncompensated samples provided by the same pump intensity. Secondly, the heavily compensated samples have lower laser thresholds. The CO_2 laser pump intensity, necessary to exceed the Si:P laser threshold for the 7 mm long sample from the best material, was about of 30 kW/cm^2 [11-13] at 10.6 µm line of the CO_2

 ISSN (print) 2958-8960 (online) 3006-6042

IRAQI JOURNAL OF MATERIALS
Volume (3) Issue (3) July-September 2024, pp. 17-24

laser (Fig. 7). The THz emission pulse from the Si:P laser started together with the pump pulse and had a duration of 70-100 ns, comparable with a full width of half maximum of the pump laser pulse (Fig. 8). The spectrum of the stimulated emission from the Si:P sample was measured by the FTS with a resolution of 0.2 cm^{-1} (Fig. 9). A line at 54.1 µm was recorded, which corresponds to the $2p_0 \rightarrow 1s(T_2)$ intracentre transition.

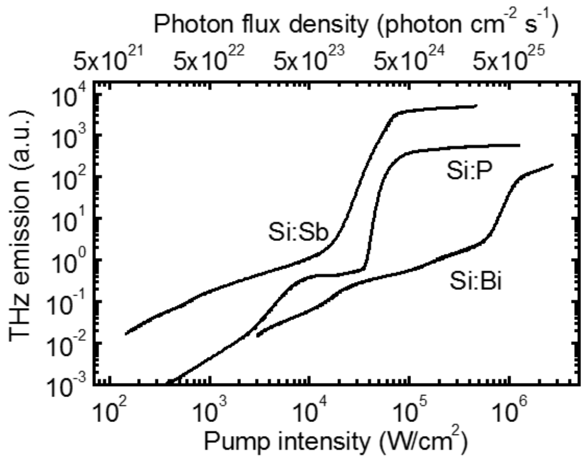

Fig. (7) The dependency of THz emission from silicon doped by different impurities

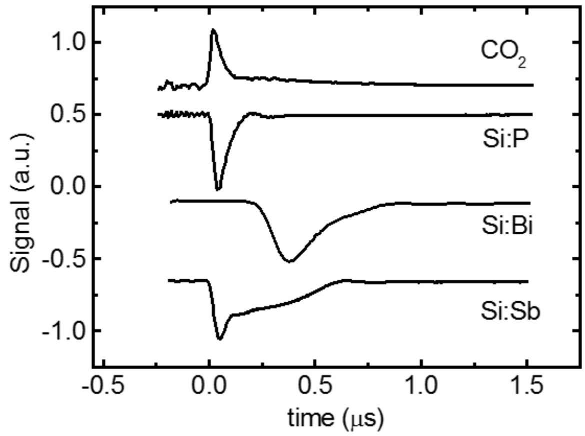

Fig. (8) The stimulated emission pulses from silicon doped by different impurities (negative signals) and CO_2 laser pulse (positive signal)

Stimulated emission from Si:Sb has been observed for the pump photon flux density higher than 10^{24} photons×cm^{-2}×s^{-1} (20 kW×cm^{-2}) for the 9.6 µm pump line (Fig. 7). Pumping by a line from the 10 µm band of CO_2 laser emission band requires a factor of 1.5-2 higher photon flux density to reach the laser threshold. This difference is caused by the different lattice absorption of the pump emission: 0.3 cm^{-1} and 1.1 cm^{-1} for 9.6 µm and 10.6 µm pump lines correspondingly [15]. The pulse shapes of the pump laser and the THz Si:Sb laser are presented in Fig. (8). The Si:Sb stimulated emission spectrum was measured by the FTS with a resolution of 0.2 cm^{-1} (Fig. 9). The spectrum consists of a single line at 171.8 cm^{-1} (5.15 THz or 58.2 µm). The interesting feature of the Si:Sb in comparison with the Si:P laser is that it ends on the $1s(T_2:\Gamma_8)$ quadruplet state. The spin-orbit coupling splits the $1s(T_2)$ state into the doublet $1s(T_2:\Gamma_7)$ and quadruplet $1s(T_2:\Gamma_8)$, separated with 0.3 meV energy spacing,, since Sb has a higher atomic number than that of P impurity centres.

In the Si:Bi samples a stimulated emission effect was observed for doping concentration in the range of N_{Bi}=(6-12)×10^{15} cm^{-3}. The CO_2 laser pump threshold intensity for Si:Bi lasing was 100-300 kW×cm^{-2} at the pump wavelength of 9.6 µm (photon flux density of (5-15)×10^{25} quantum×cm^{-2}×s^{-1}) [13,14]. Pumping by a line from the 10 µm band of the CO_2 laser required a factor ~2 higher power and exhibits the lower output signal and the longer delay of the lasing pulse. The stimulated emission pulse appears always with an essential time delay, 50-200 ns, (Fig. 8) after the peak of the pump laser pulse, while the spontaneous emission has no such a delay for all pump frequencies. Two strong emission lines, having the relatively low laser thresholds, and corresponding the $2p_{\pm} \rightarrow \{1s(E),\ 1s(T_2{:}\Gamma_8)\}$ transitions were registered in the Si:Bi spectra under the pumping by of the CO_2 laser (Fig. 9).

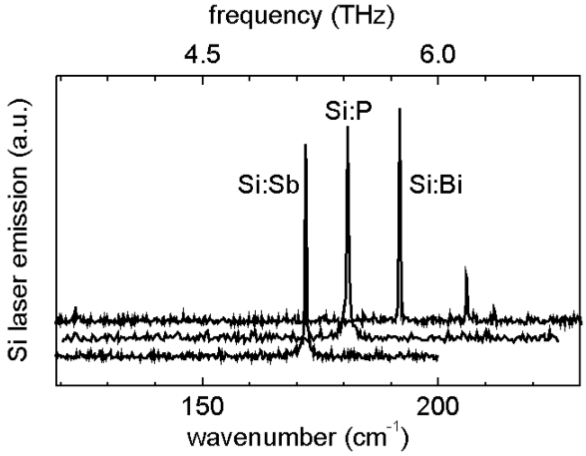

Fig. (9) The spectra of stimulated emission from silicon doped by different impurities

3. Conclusion

The influence of the nonequilibrium phonons on the populations of the working states in Si:Bi appear due to the bottled-neck effect in the decay of *TA* (≈ 20 meV) acoustic phonons. Additionally, it should be pointed out that the times of life of the $1s(E)$, $1s(T_2)$ laser states have been estimated in the simplified model using hydrogen-like eigenfunctions. This has to be defined more exactly. Also it is important to take into account the possibility of the reabsorption on the $2p_0 \rightarrow 1s(A_1)$ transition of the emitted *TO* intervalley optical phonons by Bi centres before they decay into the acoustic phonons. The latter can increase the time of life of the $2p_0$ state. The frequency coverage might be extended also by using other dopants such as As and Li. Si lasers covering 5-6 THz region with a tunability of about 1% are expected to be feasible.

References

[1] A.A. Andronov et al., "Amplification of Far-Infrared Radiation in Germanium During the Population Inversion of Hot Holes", JETP. Lett., 30 (1979) 551-555.
[2] L.S. Mazov and I.M. Nefedov, "Numerical Computation of Holes Population Inversion and FIR Amplification in Silicon", in A.A. Andronov (eds) Submillimeter Wave Lasers in Semiconductors Using Hot Holes, IAP AS, Gorky, (1986) pp. 153-166.
[3] A.V. Muravjov et al., "Amplification of Far-Infrared Radiation on Light Hole Cyclotron Resonance in Silicon in Crossed Electric and Magnetic Fields", in M. von Ortenberg and H.-U. Müller (eds) Proc. of 21th Int. Conf. on Infrared and Millimeter Waves, Berlin, CTh11 (1996).
[4] A.V. Muravjov et al., "Population Inversion of Landau Levels in the Valence Band in Crossed Electric and Magnetic Fields", phys. stat. sol. (b), 205 (1998) 575-585.
[5] A.A. Andronov et al., "Stimulated Emission in the Long-Wavelength IR Region from Hot Holes in Ge in Crossed Electric and Magnetic Fields", JETP. Lett., 40 (1984) 804-806.
[6] Y.L. Ivanov, "Generation of Cyclotron Radiation by Light Holes in Germanium", Opt. Quant. Elect., 23 (1991) S253-S265.
[7] V.N. Shastin, "Far-Infrared Active Media Based on Inraband and Shallow Impurity States Transitions in Si", in M. von Ortenberg and H.-U. Müller (eds) Proc. of 21th Int. Conf. on Infrared and Millimeter Waves, Berlin, CT2 (1996).
[8] E.E. Orlova and V.N. Shastin, "Inverse Population of Bismuth Donor Excited States and FIR Amplification in Silicon Under of Optical in Si", in M. von Ortenberg and H.-U. Müller (eds) Proc. of 21th Int. Conf. on Infrared and Millimeter Waves, Berlin, CTh4 (1996).
[9] E.E. Orlova, "Nonequilibrium Population of Shallow Impurity States in Semiconductors and Amplification of Far-Infrared Radiation", Ph.D. thesis, Institute for Physics of Microstructures RAS, Nizhny Novgorod, 128 Pages (2002).
[10] E.E. Orlova, "Longliving shallow donor states in silicon-life time calculation", in J.H. Davies and A.R. Long (eds) Proc. of 26th Int. Conf. on the Physics of Semiconductors, 29 July-2 August (2002), Cambridge, 3, p. 123.
[11] S.G. Pavlov et al., "Stimulated emission from donor transitions in silicon", Phys. Rev. Lett., 84 (2000) 5220-5223.
[12] T.O. Klaassen et al., "The emission spectra of optically pumped Si-based THz lasers", in M. Chamberlain et. al (eds) Proc. of 2002 IEEE Tenth Int. Conf. on Terahertz Electronics, (2002) pp. 89-90.
[13] H.-W. Hübers et al., "Terahertz emission spectra of optically pumped silicon lasers", phys. Stat. sol. (b), 233 (2002) 191-196.
[14] S.G. Pavlov et al., "Far-infrared stimulated emission from optically excited bismuth donors in silicon", Appl. Phys. Lett., 80 (2002) 4717-4719.
[15] S.G. Pavlov et al., "Terahertz optically pumped Si:Sb laser", J. Appl. Phys., 92 (2002) 5632.
[16] A.K. Ramdas and S. Rodriguez, "Spectroscopy of the solid-state analogues of the hydrogen atom: donors and acceptors in semiconductors", Reports on Prog. in Phys., 44 (1981) 1297-1387.

[17] T.G. Castner, "Raman spin-lattice relaxation of shallow donors in silicon", Phys. Rev., 130 (1963) 58-75.
[18] E.M. Gershenzon, A.P. Mel'nikov and R.I. Rabinovich, "H^- like impurity centers, molecular complexes and electron delocalization in semiconductors", in A.L. Efros and M. Pollak (eds.) *Electron-Electron Interactions in Disordered Systems*, Elsevier Science Publishers, Amsterdam, (1985) pp. 483-554.
[19] N.R. Battler, P. Fisher and A.K. Ramdas, "Excitation spectrum of bismuth donors in silicon", Phys. Rev. B, **12** (1975) 3200-3209.
[20] V.N. Abakumov, V.I. Perel and I.N. Yassievich, **"Nonradiative Recombination in Semiconductors"**, North-Holland Publ. Co. (Oxford, 1991).
[21] I.M. Gres'kov et al., "Influence of growth defects on the electrical properties of radiation-doped silicon", Sov. Phys. – Semicond., 12 (1978) 1118-1120.